Absence of Myocardial Thyroid Hormone Inactivating Deiodinase Results in Restrictive Cardiomyopathy in Mice

Cintia B. Ueta,* Behzad N. Oskouei,* Emerson L. Olivares,* Jose R. Pinto, Mayrin M. Correa, Gordana Simovic, Warner S. Simonides, Joshua M. Hare, and Antonio C. Bianco

Division of Endocrinology, Diabetes, and Metabolism (C.B.U., E.L.O., M.M.C., G.S., A.C.B.), Interdisciplinary Stem Cell Institute (B.N.O., J.M.H.), and Department of Molecular and Cellular Pharmacology (J.R.P.), University of Miami Miller School of Medicine, Miami, Florida 33136; and Laboratory for Physiology (W.S.S.), Institute for Cardiovascular Research, VU University Medical Center, 1081 HV Amsterdam, The Netherlands

Cardiac injury induces myocardial expression of the thyroid hormone inactivating type 3 deiodinase (D3), which in turn dampens local thyroid hormone signaling. Here, we show that the D3 gene (*Dio3*) is a tissue-specific imprinted gene in the heart, and thus, heterozygous D3 knockout (HtzD3KO) mice constitute a model of cardiac D3 inactivation in an otherwise systemically euthyroid animal. HtzD3KO newborns have normal hearts but later develop restrictive cardiomyopathy due to cardiac-specific increase in thyroid hormone signaling, including myocardial fibrosis, impaired myocardial contractility, and diastolic dysfunction. In wild-type littermates, treatment with isoproterenol-induced myocardial D3 activity and an increase in the left ventricular volumes, typical of cardiac remodeling and dilatation. Remarkably, isoproterenol-treated HtzD3KO mice experienced a further decrease in left ventricular volumes with worsening of the diastolic dysfunction and the restrictive cardiomyopathy, resulting in congestive heart failure and increased mortality. These findings reveal crucial roles for *Dio3* in heart function and remodeling, which may have pathophysiologic implications for human restrictive cardiomyopathy. **(*Molecular Endocrinology* 26: 809–818, 2012)**

The current model of thyroid hormone action holds that deiodinases mediate intracellular changes in thyroid hormone activation or deactivation that are key to many metabolic effects, regardless of plasma hormone concentrations. These enzymes, such as the type 2 deiodinase (D2), accelerate activation of T_4 to T_3 and increase local thyroid hormone action. In contrast, the type 3 deiodinase (D3) irreversibly inactivates both T_4 and T_3, thereby dampening thyroid hormone action and creating localized hypothyroidism on a cell-specific basis. Importantly, this local control of thyroid hormone action occurs without substantial changes in circulating levels of T_4 and T_3 and thus cannot be predicted by measurements of serum T_4 and/or T_3 levels (1).

There is widespread D3 expression in vertebrates during development, and D3 levels are inversely coordinated with D2, so that thyroid hormone signaling in a given tissue can be controlled according to the developmental stage (2). For example, in the 3-d period during which brown adipose tissue is formed (E16.5–E18.5), there is a simultaneous decrease in D3 and increase in D2, augmenting local T_3 concentration and thyroid hormone signaling (3). After birth, D3 expression subsides in most tissues to background levels, and D3 activity remains largely restricted to brain and skin. However, disease signals in the adult human and other mammals can reactivate D3 expression in a number of tissues (4, 5). In rat

ISSN Print 0888-8809 ISSN Online 1944-9917
Printed in U.S.A.

doi: 10.1210/me.2011-1325 Received November 17, 2011. Accepted February 9, 2012.
First Published Online March 8, 2012

* C.B.U., B.N.O., and E.L.O. contributed equally to this work.

Abbreviations: BW, Body weight; D2, type 2 deiodinase; D3, type 3 deiodinase; EE, energy expenditure; HtzD3KO, heterozygous D3 knockout; ISO, isoproterenol; IVCT, isovolumic ventricular contraction time; LV, left ventricle; MHC, myosin heavy chain; PLN, phospholamban; PV, pressure volume; RQ, respiratory quotient; RV, right ventricular; SERCA-2, sarcoplasmic reticulum Ca2-ATPase type 2; VO_2, oxygen consumption; WT, wild type.

myocardium, for example, right ventricular (RV) hypertrophy caused by pulmonary arterial hypertension results in an approximately 5-fold induction in local D3 activity, which in turn decreases sarcoplasmic reticulum Ca2-ATPase type 2 (SERCA-2)a and α-myosin heavy chain (MHC) gene expression, and increase levels of β-MHC mRNA, a pattern that is typical of the hypothyroid heart (6). In fact, D3 induction in this animal model is linked to RV hypoxia and accumulation of hypoxia inducible factor-1α, creating an anatomically specific reduction in local T_3 content and action (7). Myocardial infarction in rats (8) and mice (9) also leads to a potent chamber-specific induction of D3. In the latter model, *in vivo* measurement of thyroid hormone-dependent transcription activity in cardiomyocytes using a luciferase reporter assay revealed a marked decrease post-myocardial infarction, which was associated with a 50% decrease in left ventricle (LV) T_3 concentration (9).

The paradigm emerging from these studies is that the hypoxic myocardium banks on the D3-mediated decrease in T_3 signaling to ultimately slow down the rate of oxygen consumption (VO_2); it is not clear yet whether local hypothyroidism is necessary for myocardium remodeling. At the same time, the link between hypoxia and D3 induction has also been observed in cultures of hepatocytes and neurons (7, 10), suggesting that these D3-mediated changes in local thyroid hormone action constitute a broad adaptive response. In fact, a number of other disease and tissue injury models exhibit similar D3 reactivation and local down-regulation of thyroid hormone signaling, such as cerebral hypoxia, inflammation or oxidative stress, nerve injury, and liver resection-regeneration, suggesting that D3 induction in the heart is part of the hypoxia inducible factor-1α-orchestrated response generally seen in tissue injury, hypoxia, and/or ischemia (5).

The D3 gene (*Dio3*) is located in the delta-like 1 homolog-*Dio3* domain positioned on distal mouse chromosome 12 and human chromosome 14 (11). The domain contains three paternally imprinting protein-encoding genes that share common regulatory elements, delta-like 1 homolog, retrotransponson-like gene 1, and *Dio3*, *i.e.* only the paternally inherited allele is expressed. This is explained based on the differences between the chromatin structures such as degree of DNA methylation and post-translational modifications to core histone proteins. In mice, *Dio3* imprinting does not happen in all tissues, and even where it happens is not complete, with the paternal allele contributing with approximately 84% of expression in the embryo and 50–60% in the placenta (12). Here, we show that *Dio3* imprinting takes place in the mouse heart but not in the brain, and thus, the heterozygous D3 knockout (HtzD3KO) mice lends itself as a model of cardiac-specific *Dio3* inactivation. Strikingly, the myocardium of 1-d-old HtzD3KO pups is normal but, as a result of the lifelong cardiac increase in thyroid hormone signaling, 4-month-old animals exhibit a unique phenotype of restrictive cardiomyopathy that includes myocardial fibrosis, impaired myocardial contractility, and diastolic dysfunction. A sympathetic overdrive with a 10-d treatment with isoproterenol (ISO) worsened this phenotype, with further reductions in the LV volumes and accentuation of the diastolic dysfunction, which caused congestive heart failure and doubled the mortality rate. In sharp contrast, wild-type (WT) siblings were able to potently reactivate myocardial D3, and cardiac remodeling took place with LV dilatation. Given that D3 reactivation is present in critically ill patients with compromised myocardial perfusion (4), the present findings may have

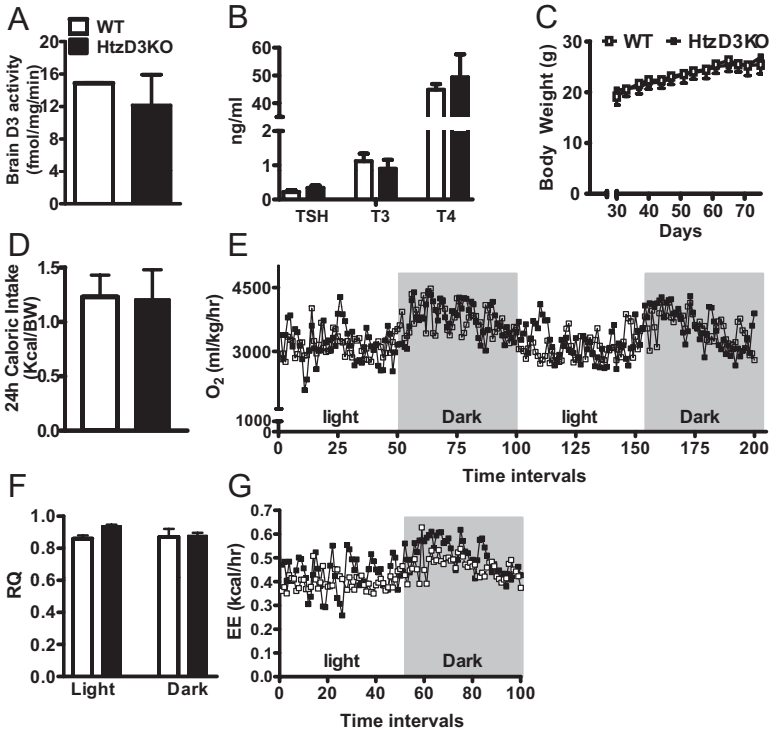

FIG. 1. HtzD3KO mice are systemically euthyroid. Cerebral cortex D3 activity (A), thyrotropin, T_3, and T_4 serum levels (B), body weight (data entries from both groups are superimposed) (C), daily caloric intake (D), VO_2 measure during 48-h period (E), 24-h RQ (F), and EE (total daily EE) (G) in WT and HtzD3KO mice. *Shaded areas* indicate night time. A–G, Data are expressed as mean ± SEM of three to five animals in each group.

pathophysiologic implications for human restrictive cardiomyopathy.

Results

The HtzD3KO mouse is euthyroid

The WT heart exhibits minimal D3 activity (~0.4 fmol T_3/min·mg protein), about 40-fold less than the D3 activity found in the brain (Fig. 1A, see also Fig. 3A below). The HtzD3KO mouse has normal brain D3 activity (Fig. 1A) but lacks cardiac D3 activity (<0.15 fmol T_3/min·mg protein), indicating that the heart is one of the tissues in which *Dio3* is imprinted. Thus, the HtzD3KO mouse constitutes a suitable model of cardiac-specific *Dio3* inactivation in an otherwise systemically euthyroid mouse. Accordingly, HtzD3KO mice exhibit normal serum levels of thyrotropin, T_4 and T_3 (Fig. 1B), and growth rates (Fig. 1C) as compared with the WT siblings. In addition, HtzD3KO mice exhibit normal 24-h caloric intake (Fig. 1D), daily VO_2 (Fig. 1E), respiratory quotient (RQ) (Fig. 1F), and energy expenditure (EE) (Fig. 1G), parameters that are strongly affected by thyroid status and serum thyroid hormone levels.

The HtzD3KO heart exhibits fibrosis, decreased maximal force, and diastolic dysfunction

The neonatal (postnatal day 1) HtzD3KO heart is histologically normal (Fig. 2, A and B) with similar expression pattern of key genes as compared with WT controls (Supplemental Table 1, published on The Endocrine Soceity's Journals Online web site at http://mend.endojournals.org). However, in 4-month-old HtzD3KO mice, the LV exhibits a typical gene expression pattern of increased thyroid hormone signaling (13, 14), *i.e.* an approximately 30% increase in the α-MHC/β-MHC mRNA ratio (Supplemental Table 1). The HtzD3KO LV also exhibits approximately 35% decrease in the SERCA-2/phospholamban (PLN) mRNA ratio as well as an approximately 30% increase in uncoupling protein-2 mRNA (Supplemental Table 1). The expression of other metabolically relevant genes, such as peroxisome proliferator-activated receptor α, glucose transporter-4, glutathione peroxidase-1, was not altered in the HtzD3KO hearts (Supplemental Table 1).

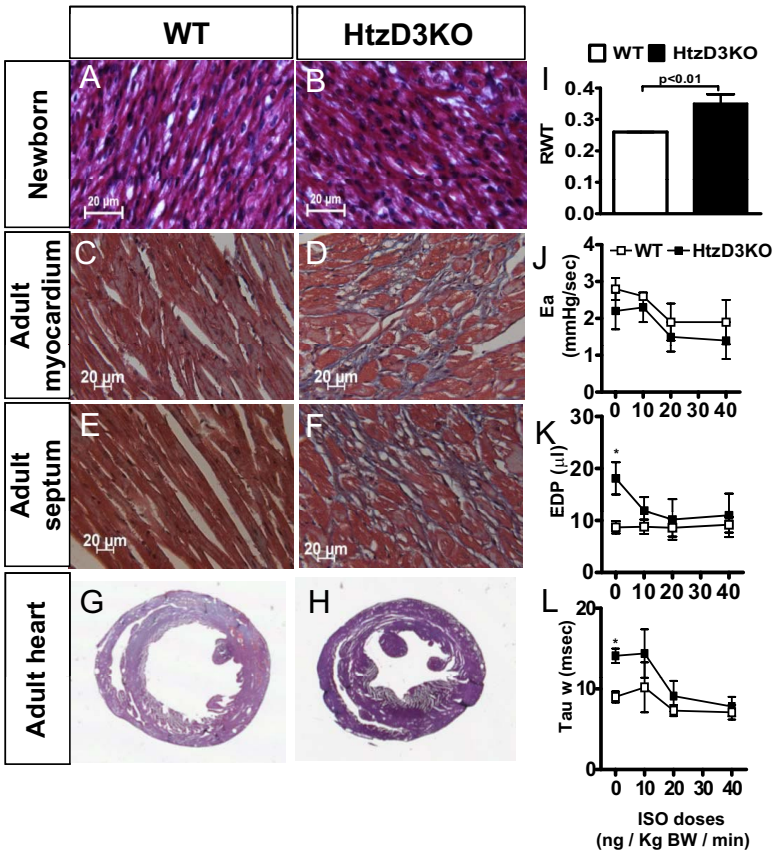

FIG. 2. Effect of life-long D3 inactivation in the heart. Representative sections of newborn LV myocardium (A and B), adult (4 month old) LV myocardium (C and D), adult cardiac septum (E and F), and heart cross-sectional analyses (G and H) of adult WT and HtzD3KO mice obtained after 20 mM KCl was infused for 10 min. *Scale bars*, 20 μm. Relative wall thickness (RWT) is the LV/RV wall ratio (I), arterial elastance (Ea) (J), end-diastolic pressure (EDP) (K), isovolumic relaxation constant (τ) (L) at baseline and during acute ISO infusion at the indicated doses. In A–L, data are expressed as mean ± SEM of three to four animals in each group; *, $P < 0.01$ *vs.* WT siblings.

To study the cardiac impact of life-long localized myocardial increase in thyroid hormone signaling, we first looked at structural parameters. Histologic examination of the HtzD3KO heart revealed that the LV myocardium (Fig. 2, C and D) and cardiac septum (Fig. 2, E and F) had substantial interstitial fibrosis, a feature previously reported in the thyrotoxic heart (15, 16). This coincides with an approximately 12-fold increase in type I collagen mRNA levels observed in the HtzD3KO LV (Supplemental Table 1). HtzD3KO hearts exhibited signs of cardiac hypertrophy (8.8 ± 0.51 *vs.* 7.2 ± 0.27 mg/mm heart weight/tibial length; n = 8; $P = 0.04$) associated with a thicker LV wall (Fig. 2, G–I). The impact of myocardial fibrosis was documented in preparations of HtzD3KO skinned papillary muscles, which exhibited about 30% decrease in calcium-activated maximal force (46 ± 1.2 *vs.* 32 ± 0.88 kN/m^2; n = 14; $P < 0.01$), with a similar stiffness

TABLE 1. Ecochardiographic and Doppler studies of WT and HtzD3KO hearts

Parameter	WT	HtzD3KO
Echocardiographic studies		
Heart rate (bpm)	480.6 ± 13	474.9 ±8.5
LV volume, diastole (μl)	67.8 ±5.6	48.3 ±4.0[a]
LV volume, systole (μl)	27.7 ±3.1	16.2 ±2.7[a]
Fractional shortening (%)	31.1 ±2.1	41.5 ±3.2[a]
Ejection fraction (%)	58.9 ±2.9	70.7 ±3.4[a]
Cardiac output (ml/min)	17.3 ±2.1	14.8 ±1.1[a]
Endocardial stroke volume (μl)	35.9 ±4.0	31.4 ±2.1[a]
Doppler studies		
E/A ratio	1.40±0.2	1.10±0.1[b]
AV peak gradient (mm Hg)	2.70±0.5	1.70±0.2[a]
Ejection time (msec)	47.5 ±2.7	46.5 ±1.2
Isovolumic contraction time (msec)	23.0 ±1.6	25.0 ±1.8
Isovolumic relaxation time (msec)	21.5 ±1.0	22.5 ±2.4
AV peak velocity (mm/sec)	807.0 ± 87	645.0 ±26[b]
MV deceleration time (msec)	20.0 ±5.0	21.0 ±2.0
Aortic acceleration time (msec)	16.0 ±2.9	15.5 ±0.9

Values are the mean ± SEM of 4–20 animals per group.

[a] $P < 0.01$ *vs.* WT, *t* test.

[b] $P < 0.05$ *vs.* WT, *t* rest.

(ranging from ~2 to 18 kN/m^2) during a 10–40% stretch ramp and myofilament calcium sensitivity (pCa_{50} = 5.71 ± 0.01 *vs.* 5.68 ± 0.01).

HtzD3KO LV exhibited impaired diastolic function as assessed by echocardiography (Table 1). Importantly LV volumes were decreased, as was the E/A (early and late/atrial) ratio, an index of diastolic chamber filling. Cardiac expression of brain natriuretic peptide mRNA levels, a sensitive marker of congestive heart failure, was not elevated in HtzD3KO LV (Supplemental Table 1).

Subsequent studies of pressure-volume (PV) relationships at baseline and during acute infusion of increasing doses of ISO indicate that the development of LV hypertrophy and fibrosis is not due to an increase in cardiovascular afterload given that arterial elastance was similar in both groups (Fig. 2J). However, the LV diastolic function assessed by the end-diastolic pressure (Fig. 2K) and by isovolumic relaxation constant (τ) (Fig. 2L) was increased in the HtzD3KO compare with WT at the baseline. Although resting parameters of contractile function and performance were similar between groups, the β-adrenergic contractile reserve was suppressed (Supplemental Fig. 1, published on The Endocrine Society's Journals Online web site at http://mend.endojournals.org), consistent with the findings in isolated muscle strips.

ISO-induced LV D3 expression promotes cardiac-specific hypothyroidism

We next extended our analysis and tested the consequences of absence of cardiac D3 during adrenergic overdrive, a recognized model of endocardial injury and diastolic dysfunction that can lead to heart failure (17). Accordingly, only in WT animals did chronic treatment with ISO stimulated D3 reactivation (~2.5-fold induction) (Fig. 3A) given that induction of *Dio3* is part of the changes in cardiac gene expression associated with ven-

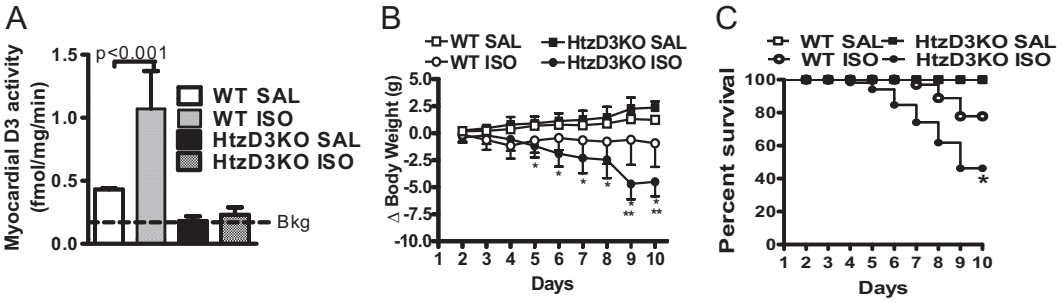

FIG. 3. Effects of treatment with ISO on myocardial D3 activity, body weight, and survival of WT and HtzD3KO mice. A, LV D3 activity after ISO or saline (SAL) injection. Bkg, Background activity. Data are expressed as mean ± SEM of 3–13 animals in each group. B, Animals were weighted daily, and variances (ΔBW) are shown. Data are expressed as mean ± SEM of 5–10 animals in each group; *, $P < 0.01$ *vs.* WT-ISO and **, $P < 0.001$ *vs.* HtzD3KO-SAL. C, Kaplan-Mayer survival plot during ISO treatment. Data are expressed as mean ± SEM of five to eight animals in each group (data entries from WT-SAL and HtzD3KO-SAL are superimposed); $P < 0.01$ *vs.* WT-ISO.

tricular hypertrophy (6, 7). In all animals, RV D3 activity was undetectable (Supplemental Fig. 2).

ISO administration minimally affected body weight in WT siblings ($P > 0.05$) (Fig. 3B), but resulted in an approximately 20% cumulative mortality rate in this group as shown by the Kaplan-Meyer survival curve (Fig. 3C). However, in the HtzD3KO animals, ISO treatment was associated with significant drop in body weight that was evident as early as d 5, reaching approximately 15% at the end of the 10-d treatment period (Fig. 3B). The cumulative mortality rate was doubled in the HtzD3KO animals, reaching about 40% (Fig. 3C). In both groups of animals, death was sudden and associated with signs of pulmonary edema and LV insufficiency.

The potent cardiac induction of D3 in the WT animals triggered by ISO (Fig. 3A) is likely to reduce local thyroid hormone signaling provided by plasma T_3. This is in contrast with the situation in the HtzD3KO heart, to which plasma T_3 has unopposed access given its lack of D3. To test this scenario, we analyzed the isovolumic ventricular contraction time (IVCT), a T_3-sensitive echocardiographic parameter, in both groups of animals before/after treatment with ISO (18). In the WT siblings, which developed the potent cardiac D3 induction (Fig. 3A), treatment with ISO caused an approximately 50% prolongation in the IVCT (Fig. 4A), a finding that is compatible with the D3-mediated reduction in thyroid hormone signaling. However, besides T_3, there are other potential regulators of this parameter, particularly in the context of ISO-induced cardiac hypertrophy. Thus, the T_3 dependency of these changes was established in the HtzD3KO animals, in which there was no induction of D3, and no ISO-induced changes in IVCT were observed (Fig. 4A). At the same time, the isovolumic ventricular relaxation time remained stable in all groups during treatment with ISO (Fig. 4B).

The changes in the myocardial α-MHC/β-MHC ratio correlated only in part with the observed D3-induced modifications in thyroid hormone signaling, given that in the failing heart, there is a natural shift in MHC isoform content from α-MHC to β-MHC and a decrease in the SERCA-2/PLN ratio (13). Thus, in ISO-treated WT siblings, induction of D3 correlated well with a reduction in α-MHC mRNA (1.02 ± 0.02 *vs.* 0.81 ± 0.02, $P < 0.001$; n = 3) and elevation in β-MHC (1.05 ± 0.02 *vs.* 1.23 ± 0.02, $P < 0.003$; n = 3). Furthermore, there was no significant decrease in α-MHC mRNA (1.23 ± 0.02 *vs.* 1.13 ± 0.005, not significant; n = 3) in ISO-treated HtzD3KO animals. Nevertheless, the α-MHC/β-MHC ratio was reduced as in the WT siblings largely due to a marked elevation in β-MHC mRNA (0.98 ± 0.02 *vs.* 0.64 ± 0.64, $P < 0.05$; n = 3). SERCA-2 mRNA levels were not affected by treatment with ISO but SERCA-2/PLN ratio was, dropping about 30% only in the ISO-treated HtzD3KO animals (1.3 ± 0.03 *vs.* 0.96 ± 0.001, $P < 0.0003$; n = 3). Changes in thyroid hormone signaling and gene expression profiles were chamber specific, given that α-MHC/β-MHC and SERCA-2/PLN ratios remained unaffected in the RV of ISO-treated animals (Supplemental Fig. 2).

In WT animals, 10-d treatment with ISO reduced serum T_4 (T_4, 45 ± 2.1 *vs.* 23 ± 1.7 ng/ml; n = 3; $P < 0.001$ by ANOVA) and increase serum T_3 (T_3, 1.06 ± 0.04 *vs.* 1.35 ± 0.02 ng/ml; n = 5; $P < 0.001$), which reflects accelerated D2-mediated conversion of T_4 to T_3, a cAMP-dependent pathway. In the HtzD3KO animals, the interpretation

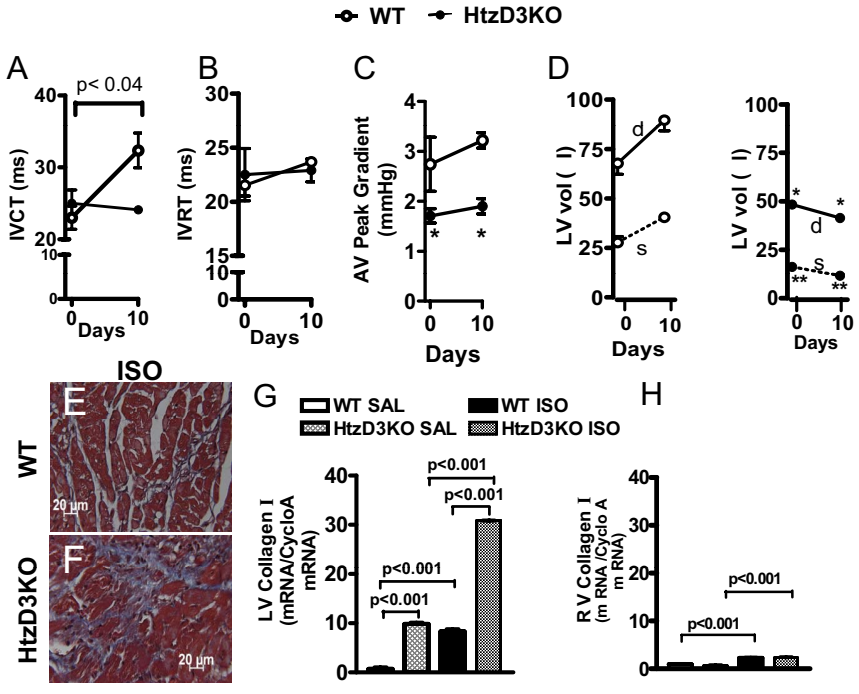

FIG. 4. Cardiac function and the impact of ISO treatment in WT and HtzD3KO mice. IVCT (A), isovolumic ventricular relaxation time (IVRT) (B), and aortic valve (AV) (C) peak gradient as assessed by Doppler at baseline and after 10 d of treatment with ISO; *, $P < 0.01$ *vs.* WT siblings. D, LV volumes (LV vol) detailed as end-diastolic volume (d) and end-systolic volume (s) as assessed by echocardiography at baseline and after 10 d of treatment with ISO; *, $P < 0.01$ *vs.* WT siblings end-diastolic volume and **, $P < 0.0003$ *vs.* WT sibling end-systolic volume. E and F, Representative histological sections of LV myocardium from WT and HtzD3KO mice after ISO treatment. *Scale bars*, 20 μm. Myocardial collagen I mRNA levels in the LV (G) and RV (H). In A—H, data are expressed as mean ± SEM of three to five animals in each group.

of the thyroid function tests is complicated by the weight loss and illness exhibited by these animals (Fig. 3, B and C). In these animals, both serum T_4 (49 ± 8.3 *vs.* 16 ± 2.7 ng/ml; n = 3; $P < 0.001$ by ANOVA) and serum T_3 (0.90 ± 0.04 *vs.* 0.77 ± 0.04 ng/ml; n = 5; $P < 0.05$ by ANOVA) were reduced by treatment with ISO.

The HtzD3KO mouse develops accentuation of restrictive cardiomyopathy during ISO-induced cardiac hypertrophy

To document this further, we used echocardiography and Doppler studies and examined the hearts of the surviving animals at the end of the 10-d ISO treatment, focusing on the LV volumes during the cardiac cycle (Fig. 4). In the WT siblings, the aortic valve peak gradient, which reflects the pressure gradient between the LV and the aorta, was not affected by treatment with ISO in either group, but this parameter was significantly greater in the WT siblings as compared with the HtzD3KO mice (Fig. 4C).

In addition, at baseline, the end-diastolic and end-systolic LV volumes were decreased in the HtzD3KO animals compare with WT siblings, indicating a decrease in LV dimensions (Fig. 4D). In the WT siblings, treatment with ISO increased the end-diastolic and end-systolic LV volumes (Fig. 4D), indicating cardiac remodeling and dilatation. In sharp contrast, in the htzD3KO animals, treatment with ISO decreased both the end-diastolic and the end-systolic ventricular volumes (Fig. 4D), indicating an accentuation of the restrictive cardiomyopathy.

The necropsy of these animals revealed that in both groups treatment with ISO increased heart weight, albeit more pronounced in the HtzD3KO animals (~35 *vs.* ~50% after correction for tibial length) (Supplemental Fig. 3A). At the same time, only in the HtzD3KO animals did ISO treatment result in a heavier lung (Supplemental Fig. 3B) and an approximately 3.5-fold increase in brain natriuretic peptide mRNA levels (Supplemental Fig. 3C), consistent with congestive heart failure. On the other hand, ventricular atrial natriuretic peptide mRNA levels were unaffected (Supplemental Fig. 3D), and liver weight remained similar in all groups, suggesting no or minimal involvement of the RV function (Supplemental Fig. 3E).

There was clear evidence of myocardial fibrosis in the ISO-treated WT siblings (Fig. 4E), whereas the fibrosis observed at baseline in the HtzD3KO animals did seem to intensify further by ISO (Fig. 2, D and F, *vs.* Fig. 4F). These data were largely confirmed by measuring myocardium collagen I mRNA levels by RT-PCR (Fig. 4G). In all groups and times, induction of type I collagen expression was minimal in the RV (Fig. 4H).

Analysis of the skinned cardiac fiber and gene expression profile explain diastolic dysfunction in HtzD3 heart

To understand the nature of the diastolic dysfunction in the ISO-treated HtzD3KO hearts, skinned cardiac fibers were studied *in situ*. Treatment with ISO decreased about 30% the calcium-activated maximal force (Fig. 5A) in the WT fibers, reaching the levels seen in the HtzD3KO. At the same time, both WT and HtzD3KO siblings exhibited a similar increase in basal force as a function of fiber stretch (stiffness), which ranged from about 2 to 50 kN/m^2 (Fig. 5B). The assessment of myofilament calcium sensitivity revealed a leftward shift in the ISO-treated HtzD3KO animals, a typical alteration ob-

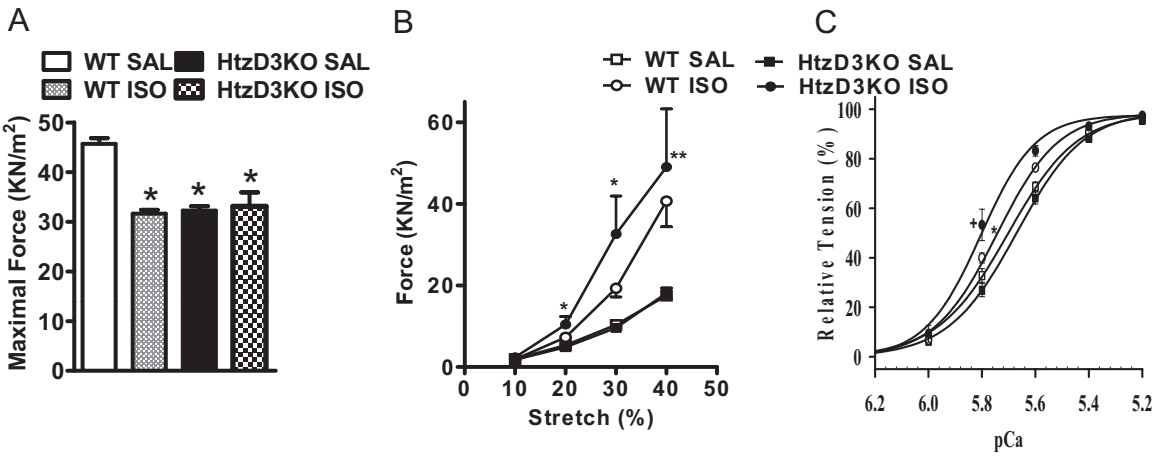

FIG. 5. Functional studies in skinned cardiac fibers of WT and HtzD3KO mice treated with ISO. A, Maximal force (kN/m^2) developed at maximal Ca^{2+} concentrations (pCa 4.0); *, $P < 0.001$ *vs.* WT-saline (SAL). B, Skinned fiber resistance to different stretch levels under resting conditions (pCa 8.0); *, $P < 0.001$ *vs.* HtzD3KO-SAL and **, $P < 0.01$ *vs.* WT-ISO. C, Ca^{2+} dependence of force development; the pCa_{50} (Ca^{2+} concentration needed to reach 50% of the maximum force) and n_{Hill} (index of thin filament cooperativity) values are: 5.7 ± 0.01 and 3.5 ± 0.11, 5.8 ± 0.01 and 3.9 ± 0.14, 5.7 ± 0.01 and 3.6 ± 0.20, and 5.8 ± 0.02 and 4.8 ± 0.52 for WT-SAL, WT-ISO, HtzD3KO-SAL, and HtzD3KO-ISO, respectively. Data are expressed as mean ± SEM of 12–14 data points in each group.

served during hypertrophic cardiomyopathy (Fig. 5C) (19).

Furthermore, the analyses of key myocardium mRNA also indicated a contrasting metabolic profile between WT and HtzD3KO animals after treatment with ISO. Although ISO treatment increased by 3- to 4-fold uncoupling protein-2 and GPX-1 (response to oxidative stress), Glut-4 (glycolysis), and PPARα (α-oxidation) mRNA levels in WT animals, all of these mRNA were decreased by 3- to 4-fold in the HtzD3KO animals, suggesting a maladaptive process (Supplemental Fig. 4).

Discussion

LV hypertrophy is widespread, affecting more than 15% of the United States adult population. It is progressive, and its prevalence increases with age, affecting more than one-third of individuals over the age of 70 (20). Although we do not understand fully the molecular underpinnings of LV hypertrophy, it is remarkable that D3-mediated cardiac-specific hypothyroidism rises as a common denominator and important feature in cardiac remodeling. In addition, other mechanisms to decrease myocardial thyroid hormone signaling that result in a hypothyroid-like mRNA phenotype have been reported during cardiac remodeling, including a decrease in thyroid hormone receptor expression in two rat models of cardiac hypertrophy [voluntary wheel running for 10 wk in adult male Wistar rats or ascending aortic constriction (pressure gradient $\approx$75 mm Hg) for 4 wk] (21). The most striking finding in the present study, however, was the contrasting phenotype caused by the absence of myocardial D3 during adrenergic overdrive (Fig. 4D). Although ISO-treated WT animals develop an enlarged LV, the HtzD3KO animals responded by reducing their LV volumes even further, worsening the restrictive cardiomyopathy and diastolic dysfunction, leading to congestive heart failure (Supplemental Fig. 3, B and C) and increased mortality (Fig. 3C). Thus, HtzD3KO animals have limited ability of cardiac remodeling during adrenergic overdrive likely as a result of the heart's inability to create localized hypothyroidism. Of note, an additional contributing factor to the poor performance exhibited by the HtzD3KO heart is likely to be the baseline cardiac fibrosis already present before ISO treatment was initiated, which is the result of long-term D3 deficiency in the HtzD3KO heart. Collectively, these data constitute strong objective evidence that myocardial D3 reactivation during adrenergic overdrive is adaptive, the absence of which leads to pathological myocardium remodeling.

The presence of myocardium fibrosis (Fig. 2, D and F) with decreased calcium-activated maximal force, LV hypertrophy (Fig. 2, G–I), and diastolic dysfunction (Fig. 2, K and L) underlie a state of restrictive cardiomyopathy in the HtzD3KO mice, revealing an critical role played by D3 in the normal myocardium. The implication of these findings is that the very low level of D3 activity present in the normal heart provides a physiological state of localized hypothyroidism, which the present data indicate is physiologically relevant. Although LV T_3 concentrations were not measured in the present experiments, the relative increase in thyroid hormone signaling is supported by the typical gene expression profile of the HtzD3KO myocardium (Supplemental Table 1) (13), including elevations in the α-MHC/β-MHC and SERCA-2/PLN ratios, despite normal serum T_3. Although of course we cannot discard that the fibrosis *per se* initiated such changes in gene expression, the consistent modification of four different T_3-responsive genes points toward enhanced T_3 signaling. Alternatively, it is conceivable that D3 expression in the "normal" myocardium reflects a small number of cardiomyocytes that are injured or damaged at any given time and are undergoing a remodeling process that requires induction of D3. These areas would thus account for what seems like global low level D3 expression.

Of note, LV afterload was similar between the WT and HtzD3KO animals (Fig. 2J), strongly suggesting that reactive hypertrophy is not operative in the D3KO mice. Thus, it is likely that this relative increase in thyroid hormone signaling underlies the myocardial fibrosis in these animals, given previous reports of myocardial fibrosis in thyrotoxic patients (15, 16). In turn, the fibrosis explains the decreased performance of the HtzD3KO skinned papillary muscle preparations (Fig. 5), leading to the phenotype of restrictive cardiomyopathy. Previous attempts to promote cardiac-specific increase in thyroid hormone signaling by way of transgenic myocardial overexpression of D2 resulted in the expected increase in adrenergic signaling and T_3-dependent gene expression profile such as observed in the present studies, but myocardial fibrosis was not investigated in those studies (22, 23).

The inducible cardiac D3 activity reported in this study (observed in the ISO-treated WT animals) reached about 1 fmol/mg protein/min, a figure that is similar to all other reports of inducible cardiac D3 activity in mice and rats (6, 7, 9). As reported, at these levels of D3 activity, there is reduction of tissue T_3 levels and T_3-dependent transcription of 40–50% (7, 9), indicating that similar mechanisms are taking place in the ISO-treated animals that exhibited D3 induction. Thus, it is not surprising that in our model of ISO-induced cardiac hypertrophy, there was echocardiographic evidence of myocardium hypothy-

roidism such as approximately 60% prolongation of the IVCT (Fig. 4A). Of note, the IVCT is a reliable T_3-sensitive biological parameter that has been widely used in the clinical setting to adjust the replacement dose of levothyroxine T_4 when serum thyrotropin cannot be used, such as in patients with secondary hypothyroidism (24).

In conclusion, the heart's ability to reactivate D3 in response to injury is a critical component of a successful remodeling process. In its absence, there is restrictive cardiomyopathy that is further accentuated in response to an adrenergic overdrive. Although we do not understand the molecular underpinnings of these adaptive mechanisms, it is conceivable that a reduction in thyroid hormone signaling establishes an adaptive transcriptional footprint that is favorable to cardiac remodeling. It is fascinating that D3-mediated hypothyroidism in response to illness is not unique to the heart, being observed in other models of tissue injury and healing, including cerebral ischemia, liver resection, and nerve injury, suggesting that D3 reactivation is part of a much broader adaptive network that is set in motion in response to illness.

Materials and Methods

Mice

All studies were performed according to a protocol approved by the Animal Care and Use Committee of University of Miami in compliance with National Institutes of Health standards. All experiments were conducted in newborns (P1) or 4-month-old 129/Sv/C57 Black/6J male mice. All mice were housed under a 12-h light, 12-h dark cycle at 22 ± 1 C, kept on a chow diet and water *ad libitum*. Mice with targeted disruption of the *Dio3* gene (D3KO) were previously described (25). A colony of animals heterozygous for the D3 inactivating mutation (HtzD3KO) and WT littermates derived from a male HtzD3KO mouse was studied.

Indirect calorimetry

Indirect calorimetry (VO_2, RQ, and EE) was performed in a Comprehensive Lab Animal Monitoring System (Columbus Instruments, Columbus, OH), a computer-controlled open circuit calorimetry system, as described (26).

Treatment with ISO

This was done by sc injections of D-L ISO [100 mg/Kg body weight (BW)/d; Sigma, St. Louis, MO] or 0.9% saline for 10 d.

Transthoracic echocardiography and Doppler studies

Cardiac function was monitored by Vevo 770 imaging system (VisualSonic, Inc., Toronto, Canada) at baseline and at the end of the treatment period. Images were recorded under anesthesia with isoflurane inhalation (1%) at heart rates above 400 bpm and body temperatures of 37 ± 1 C. Heart sonographic structural parameters were determined using the M-mode and two-dimensional images. Doppler echocardiographic images of mitral and aortic valves were recorded and calculated accordingly.

PV loop

Hemodynamic evaluation using a conductance manometry catheter was done while PV loops were recorded. Under general anesthesia (1% isoflurane) mice were intubated, and the internal carotid was canulated so that a PV loop catheter (SPR 839; Millar Instruments, TX) was passed to the LV to allow steady state occlusion parameters to be recorded at baseline and also with three doses of iv ISO infusion (10, 20, and 40 ng/kg BW/min for 5 min).

Euthanasia and serum levels of thyrotropin, T_4, and T_3

At the end of the experimental periods and procedures, mice were euthanized by CO_2 asphyxiation. Blood was collected and serum levels of thyrotropin, T_4, and T_3 measured using a MILLIPLEX rat thyroid hormone panel kit as described by the manufacturer (Millipore Corp., Billerica, MA) and read on a BioPlex (Bio-Rad, Hercules, CA). Heart, lung, and liver were harvested, and organ weights were expressed as a function of the tibial length.

Histological studies

Hearts fixed in 4% paraformaldehyde and placed in a 30% sucrose solution prepared in 0.1 M phosphate buffer. Then samples were snap frozen in liquid nitrogen and stored at −80 C until further processing. Hearts were then sliced transversely (~2 mm) at papillary level, and staining was with hematoxilin and eosin as well as Masson's trichrome.

mRNA analysis

Total heart RNA was extracted using the RNeasy kit (QIAGEN Sciences, Valencia, CA), and 2.5 μg of total RNA were reverse transcribed using High Capacity cDNA Reverse Transcription kit (Applied Biosystem, Foster City, CA). Abundance of mRNA molecules of interest was measured by RT-quantitative PCR (Bio-Rad iCycler iQ Real-Time PCR Detection System). In all assays, amplification efficiency was more than 90% and r^2 more than 0.95. Results are expressed as ratios of mRNA of interest/cyclophilin A mRNA.

D3 assay using ultra performance liquid chromatography

D3 activity was measured in the hearts and brain of all animals. Frozen tissue was processed with a Tissue Tearor (BioSpec Products, Bartlesville, OK) and homogenized in 10 mM dithiothreitol and 0.25 M sucrose. D3 activity was measured as previously described (10) using 150 μg of protein homogenate incubated at 37 C with 0.1 or 100 nM 3,5,[^{125}I]3′-triiodothyronine (PerkinElmer Life and Analytical Sciences, Inc., Waltham, MA) and 30 mM dithiothreitol. Reactions were stopped by addition of methanol and the products of deiodination separated by ultra performance liquid chromatography (ACQUITY; Waters Corp., Milford, MA) and quantified by a flow scintillation analyzer (PerkinElmer, Shelton, CT).

Mouse skinned cardiac fiber preparation and measurement of the Ca^{2+} sensitivity of force development, maximal force, and resistance to stretch

Skinned papillary muscles were prepared from the LV of freshly obtained WT or HtzD3KO mouse hearts following standard protocols of the laboratory (27). Strips of LV papillary muscle were extracted and incubated in a pCa 8.0 solution containing 1% Triton X-100 and 50% glycerol at 4 C for approximately 4–6 h. Fibers were then transferred to the same solution without Triton X-100 and stored at −20 C. Mouse muscle fiber bundles with a diameter varying between 65 and 139 μm, and approximately 1.3 mm of length were attached to tweezer clips connected to a force transducer. To ensure complete membrane removal and complete access to the myofilament, the fibers were treated with pCa 8.0 containing 1% Triton X-100 for 30 min before the beginning of the experiment. To remove the excess Triton X-100 from the fibers, extensive washing was carried out with pCa 8.0, and then the functional parameters were evaluated. To determine the Ca^{2+} sensitivity of force development, the fibers were gradually exposed to solutions of increasing Ca^{2+} concentration from pCa 8.0 to 4.0. Data were analyzed using the following equation: % change in force = $100 \times [Ca^{2+}]^n/([Ca^{2+}]^n + [Ca^{2+}{}_{50}]^n)$, where $[Ca^{2+}{}_{50}]$ is the free $[Ca^{2+}]$ that produces 50% force and n is the Hill coefficient. The maximal force in kN/m^2 developed by the fibers was evaluated by incubating the fiber in pCa 4.0 solution. For the stretch-force relationship measurements, the slack length from the fiber was determined by releasing and stretching until it begins generating tension. We set this point as zero for both the passive force and starting length. After this, the fiber was consecutively stretched 10% of its original length, and the passive force in kN/m^2 was recorded. These experiments were carried out in relaxing solution (pCa 8.0).

Statistical analysis

All data were analyzed using PRISM software (GraphPad Software, Inc., San Diego, CA) and expressed as mean ± SEM. The Student's *t* test was used to compare differences between two groups. One-way ANOVA was used to compare more than two groups, followed by the Student-Newman-Keuls *post hoc* test to detect differences between groups.

Acknowledgments

We thank Jingsheng Liang for the technical assistance with the skinned fiber measurements and Dr. Valery A. Galton, Dr. Arturo Hernandez, and Dr. Donald St. Germain for kindly sharing the D3KO mouse.

Address all correspondence and requests for reprints to: Antonio C. Bianco, M.D., Ph.D., 1400 Northwest 10th Street, Dominion Towers Suite 816, Miami, Florida 33136. E-mail: abianco@deiodinase.org; or Joshua M. Hare, M.D., Biomedical Research Building, 1501 Northwest 10th Avenue, Room 824, P. O. Box 016960 (R125), Miami, Florida 33101. E-mail: jhare@med.miami.edu.

This work was supported by 1K99HL103840-01 and James and Esther King Grant 1KN13-34001 (to J.R.P.); the National Institute of Diabetes and Digestive and Kidney Diseases Research Grant 65055 (to A.C.B.); and HL-HL084275, P20 HL101443, AG025017, HL065455, and HL094849 (to J.M.H.).

Disclosure Summary: The authors have nothing to disclose.

References

1. **Gereben B, Zavacki AM, Ribich S, Kim BW, Huang SA, Simonides WS, Zeöld A, Bianco AC** 2008 Cellular and molecular basis of deiodinase-regulated thyroid hormone signaling. Endocr Rev 29: 898–938
2. **Galton VA** 2005 The roles of the iodothyronine deiodinases in mammalian development. Thyroid 15:823–834
3. **Hall JA, Ribich S, Christoffolete MA, Simovic G, Correa-Medina M, Patti ME, Bianco AC** 2010 Absence of thyroid hormone activation during development underlies a permanent defect in adaptive thermogenesis. Endocrinology 151:4573–4582
4. **Peeters RP, Wouters PJ, Kaptein E, van Toor H, Visser TJ, Van den Berghe G** 2003 Reduced activation and increased inactivation of thyroid hormone in tissues of critically ill patients. J Clin Endocrinol Metab 88:3202–3211
5. **Huang SA, Bianco AC** 2008 Reawakened interest in type III iodothyronine deiodinase in critical illness and injury. Nat Clin Pract Endocrinol Metab 4:148–155
6. **Wassen FW, Schiel AE, Kuiper GG, Kaptein E, Bakker O, Visser TJ, Simonides WS** 2002 Induction of thyroid hormone-degrading deiodinase in cardiac hypertrophy and failure. Endocrinology 143: 2812–2815
7. **Simonides WS, Mulcahey MA, Redout EM, Muller A, Zuidwijk MJ, Visser TJ, Wassen FW, Crescenzi A, da-Silva WS, Harney J, Engel FB, Obregon MJ, Larsen PR, Bianco AC, Huang SA** 2008 Hypoxia-inducible factor induces local thyroid hormone inactivation during hypoxic-ischemic disease in rats. J Clin Invest 118:975–983
8. **Olivares EL, Marassi MP, Fortunato RS, da Silva AC, Costa-e-Sousa RH, Araújo IG, Mattos EC, Masuda MO, Mulcahey MA, Huang SA, Bianco AC, Carvalho DP** 2007 Thyroid function disturbance and type 3 iodothyronine deiodinase induction after myocardial infarction in rats a time course study. Endocrinology 148: 4786–4792
9. **Pol CJ, Muller A, Zuidwijk MJ, van Deel ED, Kaptein E, Saba A, Marchini M, Zucchi R, Visser TJ, Paulus WJ, Duncker DJ, Simonides WS** 2011 Left-ventricular remodeling after myocardial infarction is associated with a cardiomyocyte-specific hypothyroid condition. Endocrinology 152:669–679
10. **Freitas BC, Gereben B, Castillo M, Kalló I, Zeöld A, Egri P, Liposits Z, Zavacki AM, Maciel RM, Jo S, Singru P, Sanchez E, Lechan RM, Bianco AC** 2010 Paracrine signaling by glial cell-derived triiodothyronine activates neuronal gene expression in the rodent brain and human cells. J Clin Invest 120:2206–2217
11. **da Rocha ST, Edwards CA, Ito M, Ogata T, Ferguson-Smith AC** 2008 Genomic imprinting at the mammalian Dlk1-Dio3 domain. Trends Genet 24:306–316
12. **Hagan JP, O'Neill BL, Stewart CL, Kozlov SV, Croce CM** 2009 At least ten genes define the imprinted Dlk1-Dio3 cluster on mouse chromosome 12qF1. PLoS One 4:e4352
13. **Simonides WS, van Hardeveld C** 2008 Thyroid hormone as a determinant of metabolic and contractile phenotype of skeletal muscle. Thyroid 18:205–216
14. **Klein I, Ojamaa K** 2001 Thyroid hormone and the cardiovascular system. N Engl J Med 344:501–509

15. **Sandler G, Wilson GM** 1959 The production of cardiac hypertrophy by thyroxine in the rat. Q J Exp Physiol Cogn Med Sci 44:282–289
16. **Sandler G, Wilson GM** 1959 The nature and prognosis of heart disease in thyrotoxicosis. A review of 150 patients treated with 131 I. Q J Med 28:347–369
17. **Brooks WW, Conrad CH** 2009 Isoproterenol-induced myocardial injury and diastolic dysfunction in mice: structural and functional correlates. Comp Med 59:339–343
18. **Martins MR, Doin FC, Komatsu WR, Barros-Neto TL, Moises VA, Abucham J** 2007 Growth hormone replacement improves thyroxine biological effects: implications for management of central hypothyroidism. J Clin Endocrinol Metab 92:4144–4153
19. **Willott RH, Gomes AV, Chang AN, Parvatiyar MS, Pinto JR, Potter JD** 2010 Mutations in Troponin that cause HCM, DCM AND RCM: what can we learn about thin filament function? J Mol Cell Cardiol 48:882–892
20. **Drazner MH** 2011 The progression of hypertensive heart disease. Circulation 123:327–334
21. **Kinugawa K, Yonekura K, Ribeiro RC, Eto Y, Aoyagi T, Baxter JD, Camacho SA, Bristow MR, Long CS, Simpson PC** 2001 Regulation of thyroid hormone receptor isoforms in physiological and pathological cardiac hypertrophy. Circ Res 89:591–598
22. **Trivieri MG, Oudit GY, Sah R, Kerfant BG, Sun H, Gramolini AO, Pan Y, Wickenden AD, Croteau W, Morreale de Escobar G, Pekhletski R, St Germain D, Maclennan DH, Backx PH** 2006 Cardiac-specific elevations in thyroid hormone enhance contractility and prevent pressure overload-induced cardiac dysfunction. Proc Natl Acad Sci USA 103:6043–6048
23. **Carvalho-Bianco SD, Kim BW, Zhang JX, Harney JW, Ribeiro RS, Gereben B, Bianco AC, Mende U, Larsen PR** 2004 Chronic cardiac-specific thyrotoxicosis increases myocardial β-adrenergic responsiveness. Mol Endocrinol 18:1840–1849
24. **Oliveira JH, Persani L, Beck-Peccoz P, Abucham J** 2001 Investigating the paradox of hypothyroidism and increased serum thyrotropin (TSH) levels in Sheehan's syndrome: characterization of TSH carbohydrate content and bioactivity. J Clin Endocrinol Metab 86:1694–1699
25. **Hernandez A, Martinez ME, Fiering S, Galton VA, St Germain D** 2006 Type 3 deiodinase is critical for the maturation and function of the thyroid axis. J Clin Invest 116:476–484
26. **Castillo M, Hall JA, Correa-Medina M, Ueta C, Kang HW, Cohen DE, Bianco AC** 2011 Disruption of thyroid hormone activation in type 2 deiodinase knockout mice causes obesity with glucose intolerance and liver steatosis only at thermoneutrality. Diabetes 60:1082–1089
27. **Baudenbacher F, Schober T, Pinto JR, Sidorov VY, Hilliard F, Solaro RJ, Potter JD, Knollmann BC** 2008 Myofilament Ca2+ sensitization causes susceptibility to cardiac arrhythmia in mice. J Clin Invest 118:3893–3903